

1 Spatial prediction of organic carbon in German agricultural topsoil 2 using machine learning algorithms

3 Ali Sakhaee¹, Anika Gebauer², Mareike Ließ², Axel Don¹

4 ¹Thünen Institute of Climate Smart Agriculture, Braunschweig, Germany

5 ²Department Soil System Science, Helmholtz Centre for Environmental Research – UFZ, Halle (Saale), Germany

6
7 *Correspondence to:* Ali Sakhaee (a.sakhaee@thuenen.de)

8 **Abstract**

9 As the largest terrestrial carbon pool, soil organic carbon (SOC), has the potential to influence and mitigate climate
10 change, hence the importance of SOC monitoring in the frameworks of various international treaties. High
11 resolution SOC maps are therefore required. Machine learning (ML) offers new opportunities to develop these due
12 to its ability for data mining of large datasets. The aim of this study was to apply three algorithms commonly used
13 in digital soil mapping – random forest (RF), boosted regression trees (BRT) and support vector machine for
14 regression (SVR) – on the first German Agricultural Soil Inventory to model agricultural topsoil (0-30 cm) SOC
15 content and develop a two-model approach to address the high variability of SOC in German agricultural soils.
16 Model performance is often limited by the size and quality of the soil dataset available for calibration and
17 validation. Therefore, the impact of enlarging the training data was tested by including data from the European
18 Land Use/Land Cover Area Frame Survey for agricultural sites in Germany. Nested cross-validation was
19 implemented for model evaluation and parameter tuning. Grid search and the differential evolution algorithm were
20 also applied to ensure that each algorithm was appropriately tuned. The SOC content of the German Agricultural
21 Soil Inventory was highly variable, ranging from 4 g kg⁻¹ to 480 g kg⁻¹. However, only 4% of all soils contained
22 more than 87 g kg⁻¹ SOC and were considered organic or degraded organic soils. The results showed that SVR
23 produced the best performance with an RMSE of 32 g kg⁻¹ when the algorithms were trained on the full dataset.
24 However, the average RMSE of all algorithms decreased by 34% when mineral and organic soils were modelled
25 separately, with the best result from SVR with a RMSE of 21 g kg⁻¹. The model performance was enhanced by up
26 to 1% for mineral soils and by 2% for organic soils. Despite the ability of machine learning algorithms in general
27 and SVR in particular, to model SOC on a national scale, the study showed that the most important aspect for
28 improving the model performance was to separate the modelling of mineral and organic soils.

29 **1 Introduction**

30 Soil organic carbon (SOC) is the largest terrestrial carbon pool (Wang et al., 2020) and plays an essential role in
31 agriculture. Since SOC influences various physical, chemical and biological properties of soil (Reeves, 1997),
32 numerous studies recognise it as a crucial indicator of soil quality (Castaldi et al., 2019; Meersmans et al., 2012a;
33 Reeves, 1997) and therefore its decline is identified as a threat that leads to soil degradation (Castaldi et al., 2019;
34 Poeplau et al., 2020). Moreover, when considering carbon sequestration, the SOC pool provides the option for
35 climate change mitigation (Meersmans et al., 2012a; Ward et al., 2019). SOC monitoring is therefore important in
36 the frameworks of various international treaties such as the European Union Soil Thematic Strategy and the United
37 Nations Framework Convention on Climate Change (Meersmans et al., 2012b; Poeplau et al., 2020) and there is,
38 growing interest in understanding the spatial distribution of SOC at different scales in response to an increasing

39 demand for a better assessment of SOC (Minasny et al., 2013). This is particularly important for agricultural land
40 due to its potential for carbon sequestration (Lal, 2004).

41 In digital soil mapping (DSM), a soil attribute is described by an empirical quantitative function of seven factors:
42 soil properties, climate, organisms, topography, parent material, time, and spatial position (McBratney et al.,
43 2003). This function, known as the SCORPAN model, can be applied to spatially predict the soil property of interest
44 (Minasny et al., 2013). Within this framework, machine learning algorithms aim to automatically extract
45 information from the data for predictive purposes (Behrens et al., 2005). This is of particular interest in view of
46 the recent expansion of soil databases and the vast amount of data to approximate the soil forming factors
47 (McBratney et al., 2003; Wadoux et al., 2020), thus making DSM cost-effective, time-efficient and applicable over
48 large areas with good results (Behrens and Scholten, 2006; Camera et al., 2017).

49 Despite the advantages of DSM, it is crucial to note that its application requires soil databases of an adequate
50 sample size for training and testing. Furthermore, consistent and quality-checked datasets are a prerequisite for
51 DSM. Several soil inventories and monitoring networks for SOC have been established on a national scale in
52 countries such as Sweden (Poeplau et al., 2015), France (Belon et al., 2012; Arrouays et al., 2002) Denmark
53 (Taghizadeh-Toosi et al., 2014) and Scotland (Chapman et al., 2013). However, in Germany the most critical
54 shortcomings of soil inventories concern the lack of large-scale, high-quality SOC monitoring (Wiesmeier et al.,
55 2012) with periodic and standardised sampling focused on agricultural soils (Prechtel et al., 2009). These issues
56 have now been addressed in the first German Agricultural Soil Inventory (Poeplau et al., 2020). This inventory
57 was carried out on a national scale considering a sampling depth of 1 m at 3104 sampling sites covering agricultural
58 land. Furthermore, on a European scale, the Land Use/Land Cover Area Frame Survey (LUCAS) undertaken in
59 2009 is the first harmonised topsoil survey with physico-chemical analyses of georeferenced topsoil samples from
60 23 European states (Tóth et al., 2013). Therefore, by taking advantage of DSM and of both the German Agricultural
61 Soil Inventory and LUCAS survey, it is possible to regionalise from single-point measurements to obtain high-
62 resolution cover soil data nationwide and thus provide a baseline for both SOC monitoring and environmental and
63 climatic modelling for Germany.

64 Boosted regression trees (BRT), random forest (RF) and support vector machine for regression (SVR) are among
65 the most widely used algorithms in DSM (Padarian et al., 2020). For example, Martin et al. (2014) predicted topsoil
66 SOC on a national scale for France using the BRT algorithm comparing its results when the same algorithm was
67 coupled with a geostatistical approach. They concluded that due to the large distances between sampling sites,
68 spatial autocorrelation is unlikely in most national inventories, and the BRT algorithm alone is sufficient for this
69 purpose. This algorithm has also been used on a national scale in China for data from the 1980s and 2010s in
70 order to predict topsoil SOC and its spatial-temporal change, as well as the main drivers of its variability (Wang
71 et al., 2021). RF has also become more popular in DSM due to its relative simplicity and performance. For example,
72 this algorithm was implemented to map topsoil SOC on a national scale in Madagascar and identify its main drivers
73 (Ramifehiarivo et al., 2017). Ramifehiarivo et al. (2017) concluded that the uncertainty of the map generated by
74 RF model training was lower when compared with the maps that were formerly generated for the country.
75 Moreover, this algorithm was compared with the Cubist algorithm for mapping SOC at different resolutions on a
76 regional scale in China and was found to outperform it (Li et al., 2021). Fewer studies have used SVR than RF to
77 predict SOC. Studies have mainly implemented SVR on a regional scale with a limited number of samples
78 (Forkuor et al., 2017; Were et al., 2015) or on a national scale (Switzerland) with very few samples (150 samples

79 from the European LUCAS survey) (Zhou et al., 2021). However, in a study comparing different algorithms,
80 including SVR and RF, on a continental scale and within each country in Latin America, the results indicated that
81 the best-performing algorithm varied from country to country (Guevara et al., 2018). The difference mainly
82 depended on data density, quality, representativeness and country size, which affect the heterogeneity of land use
83 and environmental conditions.

84 Another important consideration when applying machine learning is the impact of the parameter-tuning strategy
85 in algorithm performance. This is particularly crucial when the objective of the study is to compare different
86 machine learning algorithms. Although some algorithms are less sensitive to tuning, this step is more important
87 for others, particularly those with a higher number of parameters (Tziachris et al., 2020; Wadoux et al., 2020).
88 Furthermore, as algorithms differ by type of parameter, continuous or discrete, the chosen strategy should be
89 aligned with this difference (Ließ et al., 2021). For example, the performance of SVR and BRT has been shown
90 to be better and more stable when optimised by a differential evolution (DE) algorithm than tuned by grid search
91 (Zhang et al., 2011; Gebauer et al., 2020). Despite this importance, in a review of studies that have applied DSM,
92 Wadoux et al. (2020) state that almost half of them implemented parameter tuning, with grid search the most
93 common strategy applied for this purpose. This finding indicates that the role of parameter tuning and optimisation
94 is unfortunately undermined in DSM. This is particularly evident when the application of machine learning in this
95 field is compared with other fields, where various studies have shown the impact of parameter-tuning strategies
96 on the performance of algorithms such as SVR and BRT (Liang et al., 2011; Santos et al., 2021; Bhadra et al.,
97 2012; Deng et al., 2019).

98 The aims of the present study were therefore: i) to address the above-mentioned parameter-tuning issue and
99 consequently provide a true comparison of the performance of BRT, RF, and SVR in modelling the SOC contents
100 of German agricultural topsoils (0-30 cm), ii) to assess the impact of training data size by extending the data of the
101 German Agricultural Soil Inventory with LUCAS data for model calibration, and iii) to develop a two-model
102 approach to address the high variability of SOC in German agricultural soils and compare it with a single-model
103 approach.

104 **2 Materials and methods**

105 **2.1 Soil data**

106 The models were built using SOC content data from two soil inventories. The first dataset was from the German
107 Agricultural Soil Inventory, which comprise of 3104 sites collected along a grid of 8x8 km throughout Germany
108 (Poeplau et al., 2020). The sites were sampled and analysed for different soil properties, including SOC content
109 measured via dry combustion, for the upper 30 cm of the soil between 2012 and 2018. The second dataset was the
110 European LUCAS survey that provides SOC content, similarly also measured via dry combustion, with the
111 sampling depth limited to 0-20 cm (Tóth et al., 2013). For Germany, data collected on agricultural soils cover 1223
112 sites. Therefore, in order to harmonise the depths of both datasets, they were subdivided into two classes: mineral
113 and organic soils according to a SOC threshold value of 87.0 g kg⁻¹. Accordingly, all soils above this threshold
114 were considered as organic soils comprising peat soils and disturbed and degraded peat soils (Poeplau et al., 2020).
115 Linear regression functions were derived for both mineral, Eq. 1, and organic, Eq. 2, soil classes on behalf of the
116 data of the German Agricultural Soil Inventory to relate the SOC content of 0-30 cm to that of 0-20 cm. These
117 functions were then applied to the corresponding soil class from the LUCAS data in order to estimate 0-30 cm

118 topsoil SOC. The 0-30 cm LUCAS data generated and the original 0-20 cm LUCAS data were then used by each
119 algorithm to check the effect of depth extrapolation.

$$120 \quad y = 1.01 + 0.881x \quad (1)$$

$$121 \quad y = 1.6 + 1.02x \quad (2)$$

122 **2.2 Covariates**

123 Covariates from multiple sources were included to approximate the SCORPAN factors throughout Germany. In
124 the case of multiple data products for one covariate, the one with the best quality (fewer artefacts) and the highest
125 spatial resolution was added. These were then resampled in ArcGIS (ESRI, 2013) using the INSPIRE standard
126 grid at 100 m resolution (Eurostat grid generation tool for ArcGIS). The resampling method was either the nearest
127 neighbour for categorical covariates or bilinear interpolation for continuous covariates. The same INSPIRE grid
128 was also used to rasterise the vector covariates. Finally, they were stacked and overlaid on SOC databases in order
129 to extract values at the sampling points.

130 Following the SCORPAN framework, 24 covariates including x and y coordinates for spatial position were
131 compiled. In order to represent the climate factor (C factor), precipitation (DWD, 2018c), sunshine duration
132 (DWD, 2017), summer days (DWD, 2018b), and minimum temperature (DWD, 2018a) were applied according to
133 the study of Schneider et al. (2021). Using principal component analysis, these four covariates were identified to
134 be the most important out of 34 available climate factors for SOC in the German Agricultural Soil Inventory
135 dataset. Moreover, type of agricultural land use is one of the main drivers of SOC variability on a national scale
136 (Poeplau et al., 2020), therefore the land use map from the official topographic-cartographic information system
137 (BKG, 2019) with its corresponding classes according to the German Agricultural Soil Inventory was rasterised
138 and included. This is a categorical covariate, representing the organism factor of SCORPAN (O factor), which
139 distinguishes croplands from grasslands and captures their spatial distribution throughout Germany.

140 The European Digital Elevation Model (EUEM) (European Union Copernicus Land Monitoring Service, 2016)
141 with original resolution of 25 m was resampled to 100 m. Six covariates derived from the resampled layer were
142 also added to integrate the relief parameter (R factor). Slope, plan curvature and profile curvature, generated with
143 SAGA (Conrad et al., 2015), were included to capture the slope's gradient, convexity-concavity and convergence-
144 divergence. These factors influence the soil distribution throughout the landscape, e.g. affecting flow over the
145 surface, thus impacting SOC and its dynamic (Ritchie et al., 2007). Moreover, slope exposition (aspect) was
146 calculated from the EUEM as it influences soil development and subsequently affects SOC (Carter and Ciolkosz,
147 1991). The circular variable was then decomposed into northness and eastness. The Topographic Wetness Index
148 (TWI), generated on SAGA, was also added since it captures the soil moisture distribution of the landscape and
149 some studies have shown its direct correlation with SOC (Pei et al., 2010). A geomorphographic map of Germany
150 (BGR, 2007) featuring 25 geomorphic categories was also used to distinguish between four different landscape
151 areas of the country: North German lowlands, highlands, Alpine foothills and the Alps.

152 Continuing with the framework, a large-scale soil landscape unit map ("Soil Scapes in Germany") (BGR, 2008)
153 comprising 38 classes was used. This covariate divides Germany by various geo-factors that can be compiled into
154 a map with 12 soil regions. Similarly, the soil-climate region map (Roßberg et al., 2007) with 50 classes was
155 added. Moreover, the Hydrogeological unit according Hydrogeological map of Germany (BGR and SDG, 2019).

156 The hydrogeological map provides information about hydrogeologically relevant attributes including
157 consolidation, type of porosity, permeability, type of rock and geochemical classification. These categorical maps
158 were rasterised and applied to the model as the P factor of SCORPAN. Moreover, the soil factor of the framework
159 (S factor) was captured by eight covariates that represent different aspects of its properties: the map of organic
160 soils (Roßkopf et al., 2015) that distinguishes mineral soils from organic ones and explains their spatial distribution
161 throughout the country, as well as the maps of nitrogen (Ballabio et al., 2019) and clay content (Ballabio et al.,
162 2016) since they directly correlate with SOC. As nitrogen is a crucial component of soil organic matter, regions
163 with higher total nitrogen have higher SOC (Ballabio et al., 2019). Also for clay content, different studies have
164 shown that coarser soil textures tend to have a lower accumulation of SOC (Zhong et al., 2018; Hoyle et al., 2011).
165 The map of pH from Ballabio et al., (2019) was included since soil pH directly impacts microbial activities that
166 influence the turnover of soil organic matter, and consequently negatively correlates with SOC (Malik et al., 2018).
167 Furthermore, the map of available water capacity (Ballabio et al., 2016) was used as this soil property is another
168 interactive factor with SOC through plant productivity and soil texture (Burke et al., 1989; Yu et al., 2021). Soil
169 erosion is also a key factor in the SOC cycle (Li et al., 2019), which was added through the map of Europe’s net
170 soil erosion and deposition rates (Borrelli et al., 2018). Based on the WaTEM/SEDEM model, this map illustrates
171 the potential spatial displacement and transport of soil sediments due to water erosion (Borrelli et al., 2018). Figure
172 S1 provides a more detailed view for better visualisation of the covariates that were used in this study.

173 **2.3 Boosted Regression Trees**

174 Developed by Friedman et al. (2000), BRT is a tree-based algorithm that applies boosting to improve accuracy.
175 Boosting relies on combining several approximate prediction models rather than obtaining one highly accurate
176 model (Schapire, 2003). Thus, the decision trees are grown sequentially so that each decision tree predicts the
177 residual of the previous one and therefore the number of trees influences the performance of the algorithm and
178 requires tuning. However, to incorporate randomness in the model and subsequently increase the robustness of
179 performance, the trees are grown on a randomly selected data subset with no replacement (Friedman, 2002). The
180 size of this subset is controlled by a parameter known as a bag fraction. Furthermore, the contribution of each new
181 tree to the final model is regularised by learning rate, also known as shrinkage (Friedman et al., 2009). Finally, the
182 number of splits in each tree that divides the response variable into subsets is optimised by interaction depth. The
183 BRT model was built in R using the “gbm” package (Greenwell et al., 2019).

184 **2.4 Random Forest**

185 Similar to BRT, RF is another tree-based algorithm. RF uses bootstrap sampling of the dataset for growing a
186 decision tree. Subsequently, by aggregating the results of a large number of decision trees, the bias and variance
187 of the final model can be reduced (Breiman, 1999). The method of bootstrapping in conjunction with aggregating,
188 known as bagging, increases the robustness and stability of RF. However, the trees from different bootstraps may
189 form a similar structure if all covariates participate in a split of each node. Thus, the variance cannot be reduced
190 optimally through the bagging process (Kuhn and Johnson, 2013). In order to avoid this tree correlation, a random
191 subset of covariates, i.e. predictors, is selected at each split. The parameter m_{try} defines the number of predictors
192 included in this subset and should be tuned (Kuhn and Johnson, 2013). The RF algorithm was implemented by
193 setting the number of trees to 1000 and using the “Ranger” package (Wright and Ziegler, 2017) in R.

194 2.5 Support Vector Regression

195 SVR is a form of support vector machine adopted for regression. From all possible solutions, i.e. estimation
196 function, for the problem, SVR tries to obtain an estimation function that has at most ϵ deviation from the response
197 values of the training data while minimising model complexity (Smola and Schölkopf, 2004). Thus, a symmetrical
198 tolerance threshold, ϵ -insensitivity zone, is created around the estimation function (Awad and Khanna, 2015). The
199 data vectors of the samples that lie on the boundary of the ϵ -insensitivity zone are called support vectors. The
200 vector lying within the insensitivity zone are not penalized. ϵ is an optimisable parameter that controls the width
201 of ϵ -insensitivity, alters the model complexity and inversely impacts the number of support vectors (Cherkassky
202 and Ma, 2004). Moreover, the trade-off between model complexity and tolerance of ϵ deviation is controlled by a
203 parameter named C (Smola and Schölkopf, 2004; Cherkassky and Ma, 2004). Optimising the C parameter has a
204 crucial impact on SVR performance since a high C can lead to overfitting, while a low C can cause under fitting
205 (Kuhn and Johnson, 2013). The use of kernel functions makes SVR a powerful tool for nonlinear problems. By
206 implementing these functions, SVR can map the data space to a higher dimensional space where a nonlinear
207 problem can be solved linearly. In this study, the Radial Basis Function (RBF) kernel was used with gamma as its
208 tuneable parameter. This parameter affects the generalisation performance of SVR by inversely controlling the
209 influence of support vectors (Battineni et al., 2019). SVR was implemented from the package e1071 in R (Hornik
210 et al., 2021).

211 2.6 Performance evaluation

212 When training a predictive model, it is important to evaluate its generalisation performance on unseen data of the
213 same type (Hawkins et al., 2003). However, as the number of available samples is usually a limiting factor, the
214 evaluation process is often done by k-fold cross validation (CV). Therefore, the dataset is divided into k folds and
215 k – 1 folds are used for training the model and one fold for testing. This process is repeated k times so each fold
216 participate in train and test. However, to ensure the robustness of the model, each model training step should be
217 performed within the CV. This includes finding the best parameter sets for the chosen algorithm (Varma and
218 Simon, 2006). Thus, the algorithms in this study were applied on a stratified nested CV.

219 First, to ensure that the SOC distribution was represented in the CV scheme, Germany was divided into 50 strata
220 using a 100x100 km INSPIRE grid. Random samples from each stratum were then taken and compiled into a fold.
221 This procedure was continued to create five folds and was repeated five times, forming the outer loop of CV used
222 for model evaluation. A long distance between neighboring samples, 8120 m on average, prevents train and test
223 data from being spatially autocorrelated. Since the aim was to tune the algorithms' parameters, the training set of
224 the outer loop of CV was nested, creating five folds as the inner loop on which the parameter tuning was performed.
225 To evaluate the performance of algorithms, root-mean-squared error (RMSE), Eq. 3, mean absolute error (MAE),
226 Eq. 4, and mean absolute percentage error (MAPE), Eq. 5, were used. Furthermore, AIC, Eq. 6, BIC, Eq. 7, and
227 %Bias, Eq. 8, are also included in Table S2 for more detailed comparison.

$$228 \quad RMSE = \sqrt{\frac{1}{n} \sum_{i=1}^n (P_i - O_i)^2} \quad (3)$$

$$229 \quad MAE = \frac{1}{n} \sum_{i=1}^n (P_i - O_i) \quad (4)$$

$$230 \quad MAPE = \frac{1}{n} \sum_{i=1}^n \left| \frac{P_i - O_i}{O_i} \right| \times 100 \quad (5)$$

231 $AIC = -2\ln(L) + 2k$ (6)

232 $BIC = -2\ln(L) + \log(n)k$ (7)

233 $\%BIAS = \frac{1}{n} \sum_{i=1}^n \frac{(P_i - O_i)}{O_i} \times 100$ (8)

234 where n is the number of samples, L is likelihood, k is the number of parameters, and P_i and O_i are the predicted
 235 and observed values, respectively.

236 **2.6.1 Parameter tuning**

237 As mentioned previously, choosing a suitable strategy for parameter tuning is a crucial step in machine learning
 238 particularly when comparing the performance of algorithms. Therefore, two strategies were applied depending on
 239 the algorithm: 1) a grid search for RF and 2) optimisation with the DE algorithm for BRT and SVR. One major
 240 problem with applying the grid search strategy for algorithms that comprise continuous parameters such as BRT
 241 and SVR is that it is impossible to consider the whole continuous parameter space. Thus, the parameter
 242 combination for testing should be determined. However, this is not problematic for tuning RF in the present case
 243 since m_{try} is a parameter with discrete values. The DE algorithm however, is a stochastic approach to solve an
 244 optimisation problem that can be applied to both continuous and discrete parameters. This method is described in
 245 more detail by Storn & Price (1997). Therefore, SVR and BRT are optimised by this strategy as the former
 246 algorithm has continuous parameters and the latter one has both continuous and discrete parameters. For the
 247 optimisation task in the present study, the R package “DEoptim” was applied (Peterson et al., 2021). Table S1
 248 shows the parameters and their tuning range for each algorithm.

249 **2.6.2 Variable importance**

250 Variable importance was assessed by permutation (Ließ et al., 2021). The values of a particular covariate in the
 251 test set were shuffled and prior to applying the respective model to eliminate any predictor-response relationship
 252 present with regards to that predictor. The variable importance corresponds to the relative increase in the test set
 253 RMSE. This procedure was repeated 10 times for each covariate. The resulting values were averaged. Thus, the
 254 variable importance of each covariate in terms of relative change in RMSE was obtained.

255 **2.7 Modelling approaches**

256 We followed a two-by-two strategy resulting in four modelling approaches to test the performance of the
 257 algorithms (Table 1).

258 **Table 1: Modelling approaches**

	Dataset 1: German Agricultural Soil Inventory	Dataset 2: German Agricultural Soil Inventory + LUCAS
One-Model-Approach	AP1	AP1L
Two-Model-Approach	AP2	AP2L

259
 260 On the one hand, we only used the SOC data from the German Agricultural Soil Inventory and corresponding
 261 values from the covariates to train the models (AP1). Due to the high variability of SOC in the agricultural soils

262 of Germany, we then trained two separate models for organic and mineral soils (AP2) to identify whether this
263 could improve model performance. Accordingly, the German Agricultural Soil Inventory was subdivided by the
264 threshold 87 g kg^{-1} into mineral and organic soils.

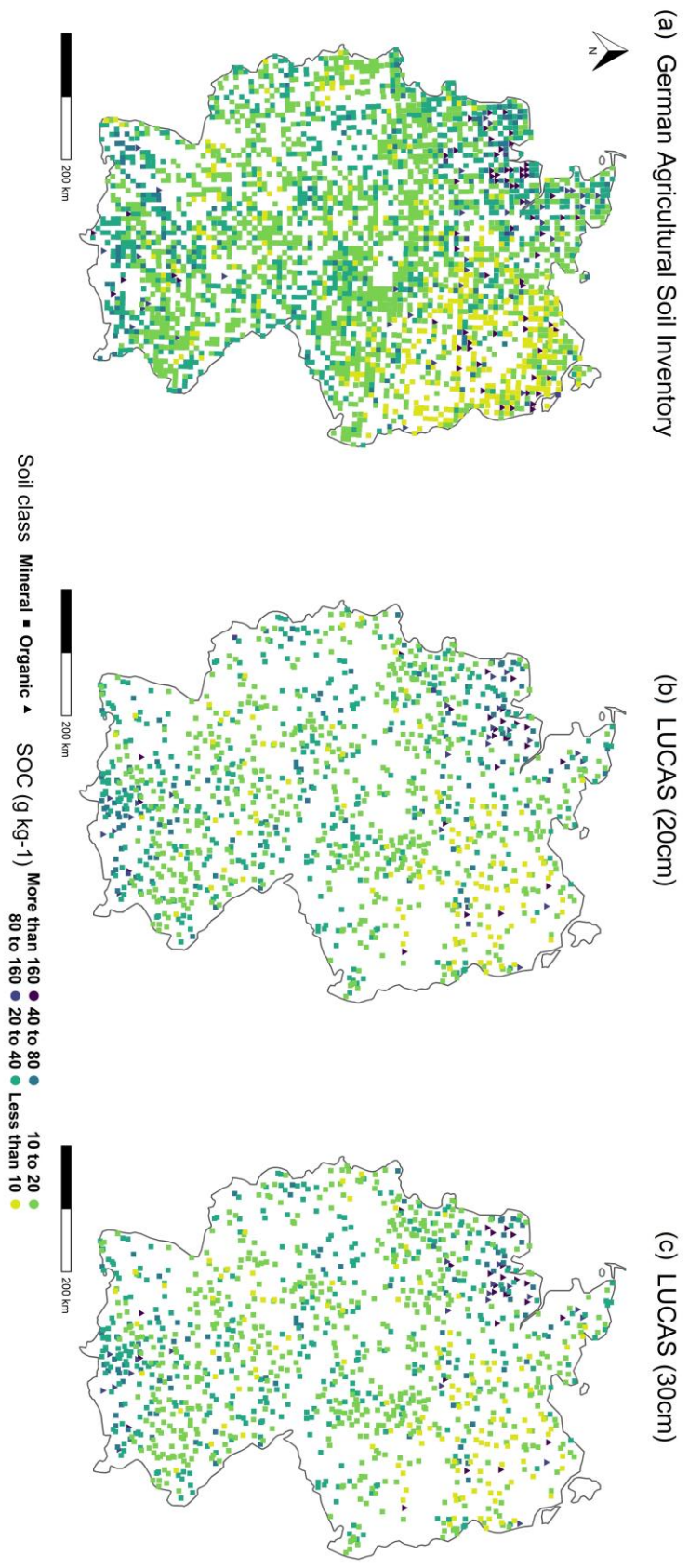
265 The impact of enlarging the training set on model performance was then examined for both, AP1 and AP2. Thus,
266 1223 depth-extrapolated samples of the LUCAS data were added to the training sets of AP1. The corresponding
267 modelling approach was named AP1L. Moreover, the same threshold (87 g kg^{-1}) was used to subdivide this dataset
268 and each soil class was included to the training set of the corresponding soil class of AP2. This modelling approach
269 was then named AP2L.

270 The test sets for the model performance evaluation remained the same for all four approaches to make the results
271 comparable. The results of the AP1 approach served as a baseline on which the model improvement for each
272 algorithm in the other approaches were assessed.

273 **3 Results and Discussion**

274 **3.1 Comparison of algorithms on the data from the German Agricultural Soil Inventory (AP1)**

275 The range of the topsoil SOC content for the German Agricultural Soil Inventory dataset was 4 g kg^{-1} to 480 g kg^{-1} ,
276 with a mean of 27 g kg^{-1} and a median of 16 g kg^{-1} . Figure 1 shows the spatial distribution of the data. For the
277 first approach (AP1), BRT, RF, and SVR were applied to model SOC using data from German Agricultural Soil
278 Inventory. The RMSE and MAPE indicated that SVR had a better general performance than the other two
279 algorithms (Fig. 2). In this respect, the RMSE of SVR was 5% lower than that from RF and 4% lower than that
280 from BRT. Furthermore, its MAPE was 3% and 7% lower than that from RF and BRT respectively. However,
281 despite the difference in overall performance, the spatial distribution of relative residuals indicated that all three
282 algorithms were less accurate in northern of Germany compared with the centre and south of the country (Fig.
283 3A). This can be explained by the characteristics of this region and its higher SOC variability. The northern part
284 of Germany is lowland dominated by a sandy soil texture from pleistocene sedimentation with geomorphological
285 structures such as ground moraines, terminal moraines and aprons (Roßkopf et al., 2015). Despite general
286 geomorphological and pedological similarities throughout the region, 1) organic soils under agricultural use are
287 mainly located in the north and 2) mineral soils with the lowest and highest SOC contents are also located in the
288 northeast and northwest respectively. Therefore, this region has the widest SOC range.



289

290 **Figure 1: Soil organic carbon content in the topsoil of two soil inventories: A) German Agricultural Soil Inventory (0-**
 291 **30 cm), B) LUCAS at its original sampling depth (0-20 cm) and C) LUCAS after depth extrapolation (0-30 cm)**



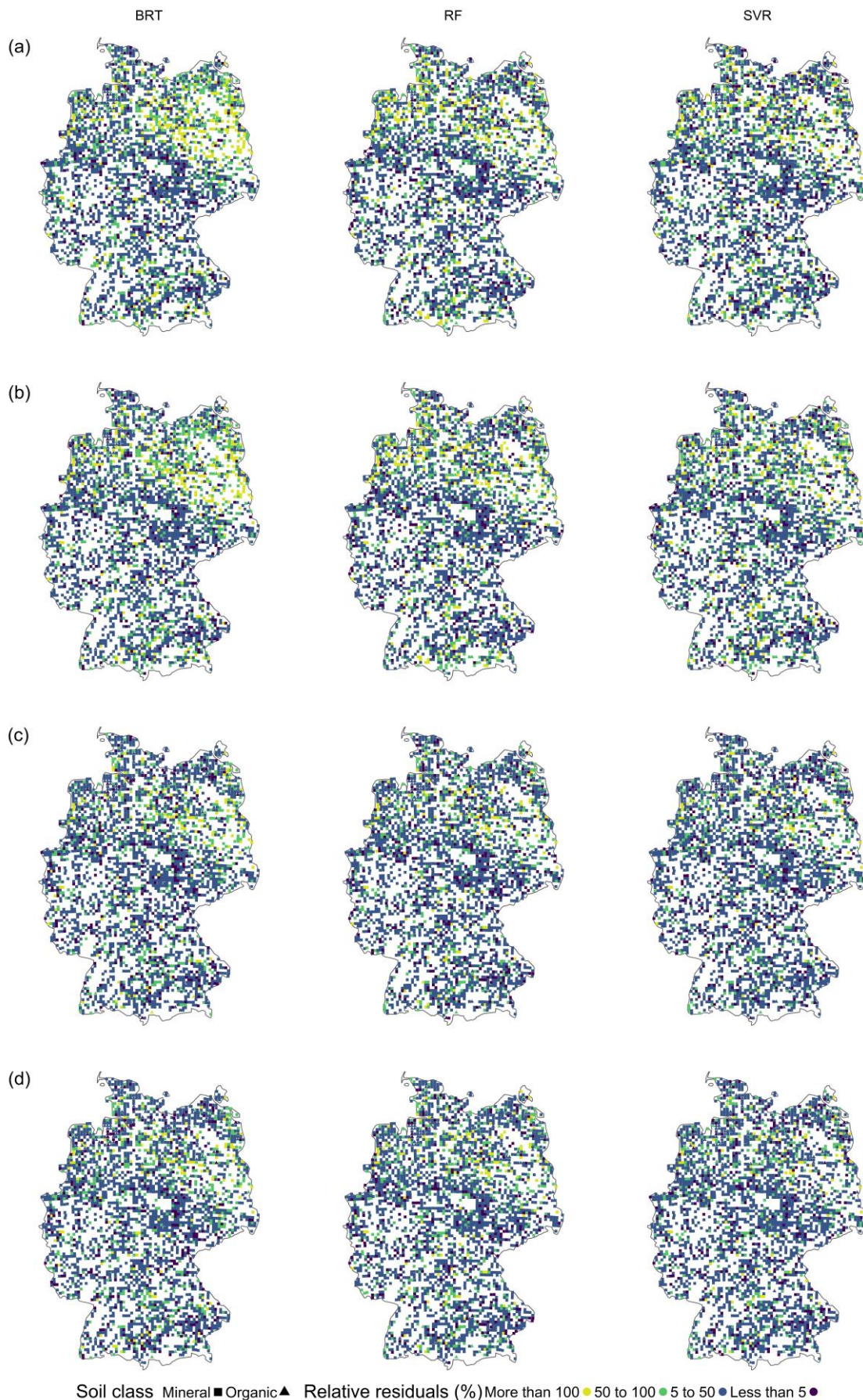
292

293 **Figure 2: Performance indicators of the three algorithms. One-model approach (without LUCAS data AP1 and with**
 294 **LUCAS data AP1L) versus the two-model approach (AP2 and AP2L) for A) RMSE (g kg^{-1}), B) MAE (g kg^{-1}) and C)**
 295 **MAPE (%). The whiskers of boxplots show 1.5 times the interquartile range. Please note that the y-axis is shortened for**
 296 **better visibility and does not display a zero. BRT = boosted regression trees, RF = random forest, and SVR = support**
 297 **vector regression.**

298 Consequently, the variable importance (Fig. 4A) indicated that the map of organic soils was the most important
 299 covariate. The value of the variable importance for this covariate was 65% in SVR, 72% in RF and 84% in BRT.
 300 These values firstly show the crucial role of the map of organic soils for the algorithms in explaining the variability
 301 of SOC and, secondly, the comparatively greater importance of this predictor and the lower variable importance
 302 of other predictors in the BRT model compared with the SVR model. Despite the importance of the organic soil
 303 map, the scatterplots (Fig. 5A) show that all three algorithms underpredicted the SOC of organic soils and had
 304 similar heteroscedasticity patterns in their residuals. Thus, while most residuals from mineral soils followed the
 305 1:1 line, they became more scattered in soils with a higher SOC content. The underprediction of SOC in organic
 306 soils can be explained by their small sample size, resulting in a dataset with a wide SOC range and a unimodal
 307 distribution that leaves these soils in the tail. Consequently, the organic soils were underrepresented and the results
 308 were systematically pulled towards mineral soils, irrespective of the choice of algorithm. Different studies have
 309 shown that predicting soil properties with mineral and organic soils combined can lead to underprediction or

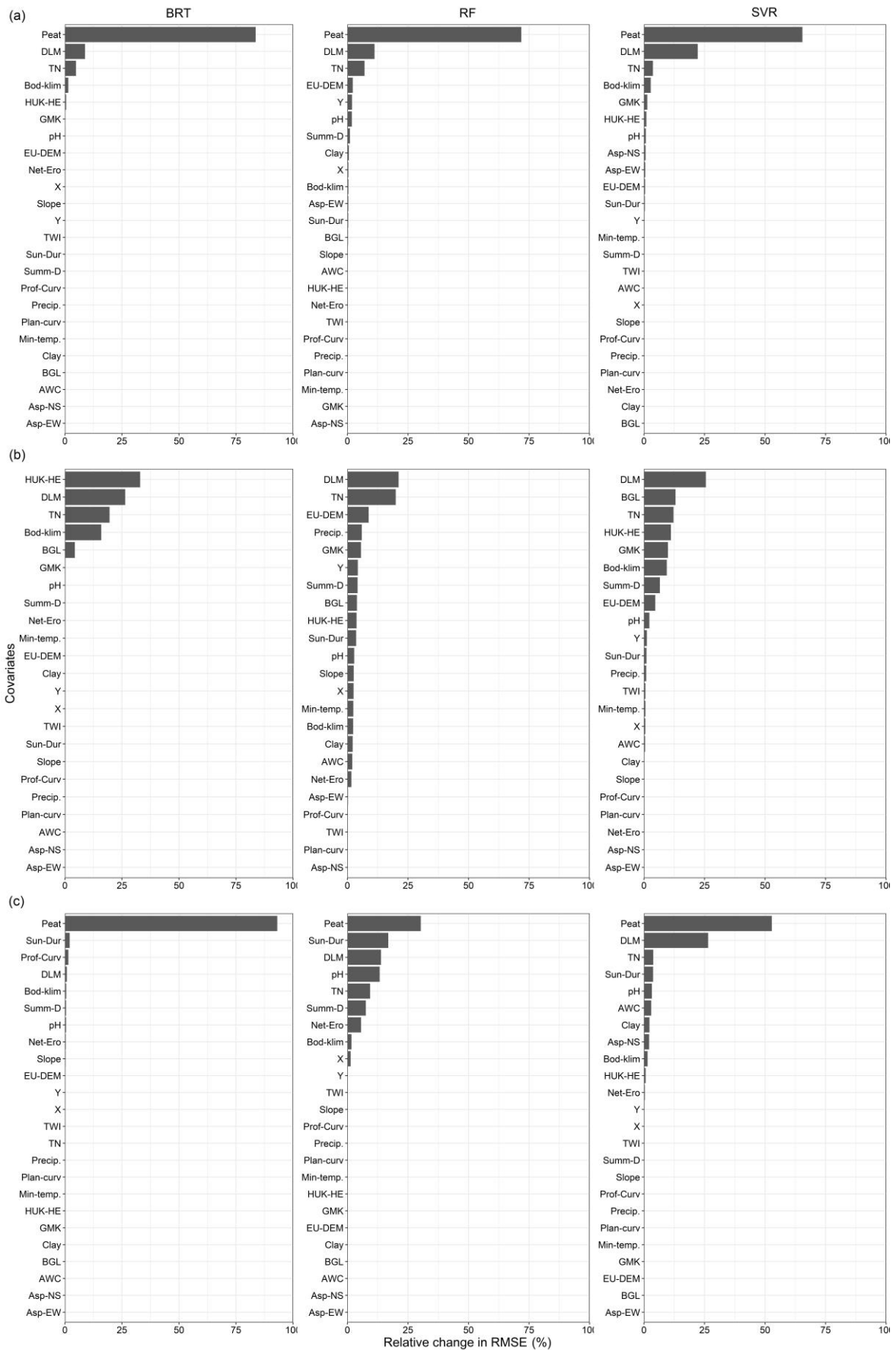
310 overprediction of one soil class, depending on the distribution of the dataset (Brogniez et al., 2015; Guio Blanco
311 et al., 2018; Mulder et al., 2016).

312 Although the map of organic soils was able to distinguish between the two soil classes, i.e. between mineral and
313 organic soil, it could not separate the mineral soils with a low SOC content in the northeast from those with a high
314 SOC content in the northwest. The spatial distribution of the residuals (Fig. 6A) showed that SVR and BRT
315 generally underpredicted the mineral soils in the northwest part of Germany, while RF overpredicted them.
316 Furthermore, unlike RF and SVR, BRT appreciably overpredicted SOC of north-east Germany's mineral soils
317 with the lowest SOC content ($<10 \text{ g kg}^{-1}$). This result indicates that the algorithms differed in their performance in
318 mineral soils. This difference was mainly due to the information they obtained from the land use map. As the
319 second most important covariate for all three algorithms (Fig. 4 A), the value for variable importance for this
320 covariate was 22% in SVR, but just 11% in RF and 9% in BRT. Thus, SVR exploits more information from this
321 covariate than RF and particularly BRT. Land use is one of the main drivers of SOC variability on a national scale
322 due to the higher SOC content in grasslands than in croplands (Poeplau et al., 2020). Therefore, this covariate was
323 able to differentiate between the soils of the northeast, which are under cropland, and those in the northwest as
324 they are more under grassland. Consequently, the reliance of BRT on the map of organic soils at the expense of
325 land use could explain why this algorithm overpredicted SOC in croplands in the northeast.



326

327 **Figure 3: Spatial distribution of relative residuals. A) AP1 approach, B) AP1L approach, C) AP2 approach and D)**
 328 **AP2L approach. BRT = boosted regression trees, RF = random forest, and SVR = support vector regression.**



329

330
331
332

Figure 4: Variable importance in terms of average relative change (%) in RMSE. A) AP1, B) mineral soil subset of AP2 and C) organic soil subset of AP2. The full name for each abbreviation is presented in Table S4. BRT = boosted regression trees, RF = random forest, and SVR = support vector regression.

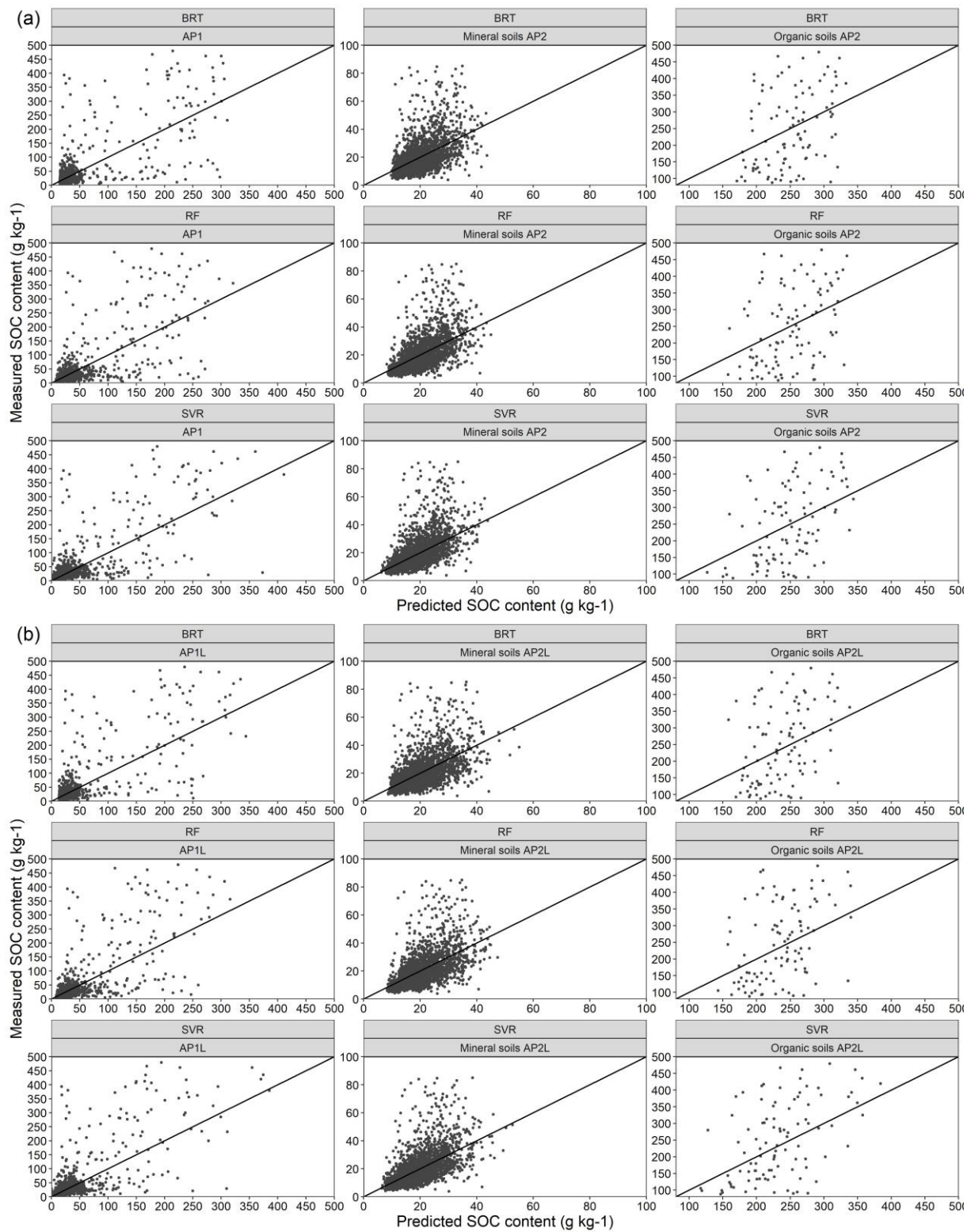
333 3.2 Enlarging the dataset with additional soil inventories (AP1L)

334 A larger soil dataset may provide additional information and consequently improve model performance. This
335 possibility was explored in the AP1L approach by adding LUCAS data. The SOC content of LUCAS data at its
336 original depth ranged from 4 g kg⁻¹ to 500 g kg⁻¹, with a mean of 30 g kg⁻¹ and a median of 18 g kg⁻¹. After
337 extrapolating the depth to 30 cm, the new range was from 5 g kg⁻¹ to 512 g kg⁻¹, with a mean of 28 g kg⁻¹ and a
338 median of 17 g kg⁻¹. The spatial distribution of LUCAS data at their original and extrapolated depth is shown in
339 Figure 1.

340 A statistical test was performed on the residuals of models built on LUCAS data with the original and extrapolated
341 depths. That was done to identify whether extrapolating the depth of LUCAS data to that of the German
342 Agricultural Soil Inventory would significantly affect model performance after their inclusion in the training set.
343 With the Shapiro-Wilk test rejecting the normality assumption of residuals of all corresponding algorithms at 20
344 cm and 30 cm, the non-parametric Kruskal-Wallis test showed no significant difference between the residuals at
345 either depth. Thus, the extrapolation of soil depth had no significant impact on data quality to regionalise SOC. As
346 a result, any further change in the performance of the algorithms after adding LUCAS data was due to enlargement
347 of the training set. The result of the algorithms at both depths can be found in the supplementary information (Fig.
348 S3).

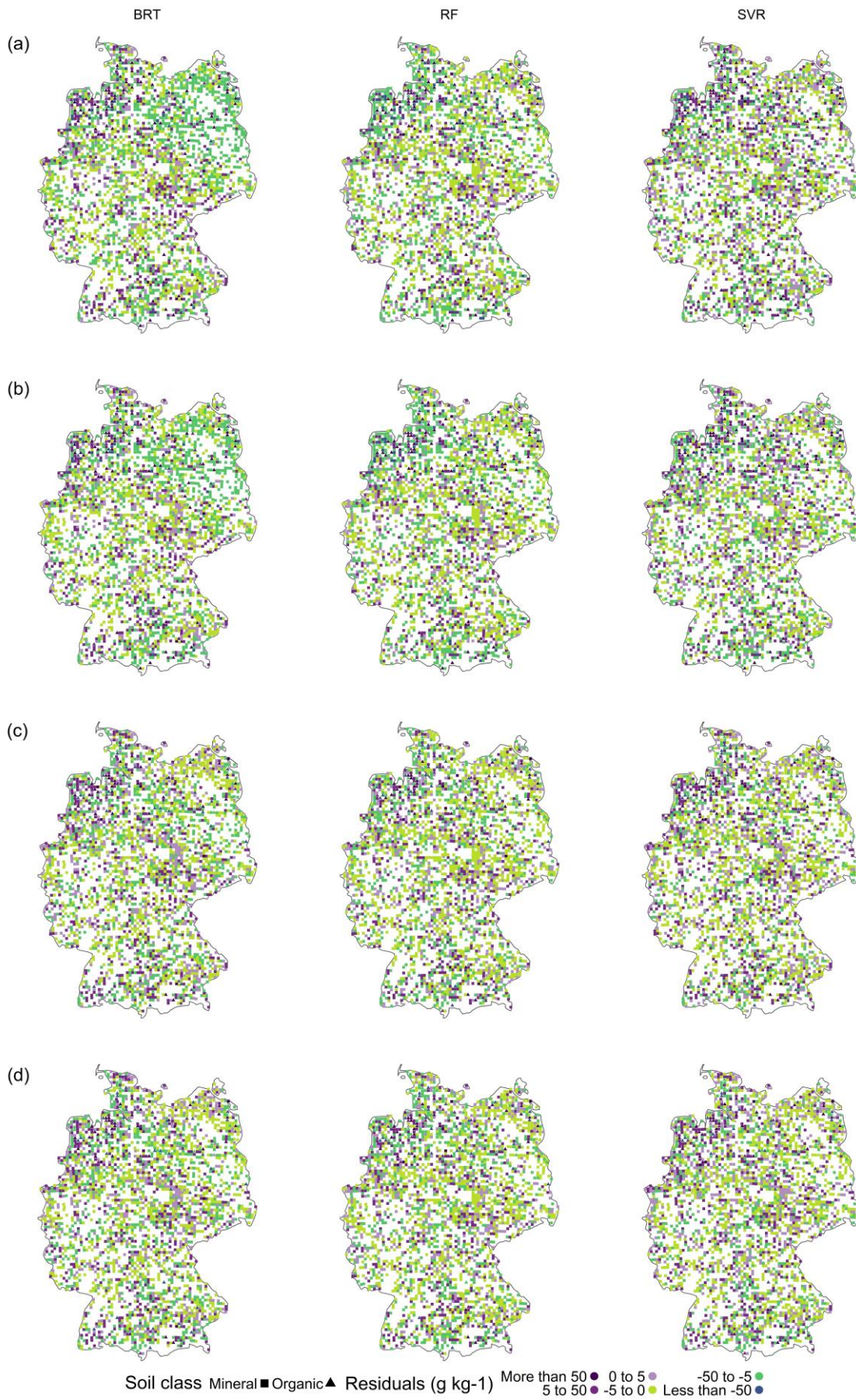
349 After enlarging the training set from 2278 to 3501 sampling points, BRT obtained the lowest RMSE (Fig. 2A1)
350 and MAE among the algorithms (Fig. 2B1). A comparison of the error metrics of corresponding algorithms from
351 the AP1 approach with those from the AP1L approach showed that BRT had the highest error reduction at 7% in
352 the MAPE and 5% in the RMSE and MAE. Furthermore, although the error metrics of RF did not improve as
353 much as those of BRT, additional training points were still beneficial for this algorithm. However, SVR did not
354 follow any systematic change under the AP1L. Despite a 2% decrease in MAPE, the RMSE increased by 3% and
355 MAE remained unchanged. To explore the potential explanation for this behaviour by SVR, the residuals of
356 mineral soils were separated from those of organic soils. Additional samples reduced the RMSE in mineral soils
357 for all algorithms by between 9% and 13%. However, this error increased by 9% in the organic subset for SVR,
358 while it increased by just 1% for RF and even decreased by 1% for BRT. This indicated that enlarging the training
359 set by data with similar characteristics had a greater influence on systematic error of the underrepresented soil
360 class in SVR. This influence is understandable when considering the higher optimised ϵ in the AP1L approach
361 compared with that of AP1 approach. The higher value of ϵ means that the hyperplane for the training set is less
362 complex (Cherkassky and Ma, 2004) and more suitable for predicting most soil samples, i.e. mineral soils. Thus,
363 when this hyperplane was fitted to the test set identical to the AP1, the generalisation performance was hindered
364 because it could not capture the variability of samples with higher SOC values, i.e. organic soils.

365 Further evaluation revealed that regardless of the change in error metrics, the relative residuals of the three
366 algorithms had a similar spatial pattern to their counterpart from AP1. Thus, they all showed lower accuracy in the
367 northern region of Germany for similar reasons (Fig. 3B). Moreover, the scatterplots had a similar pattern with
368 underpredicted organic soils (Fig. 5B). This confirmed that when organic soils are modelled with mineral soils,
369 enlarging the training set does not provide enough information for BRT or RF to capture the high variability of
370 SOC, particularly in the north of Germany.



371

372 **Figure 5: Scatterplot of residuals. A) AP1 approach and mineral and organic soils of AP2 and B) AP1L approach and**
 373 **mineral and organic soils of AP2L. BRT = boosted regression trees, RF = random forest, and SVR = support vector**
 374 **regression.**



375

376

377

Figure 6: Spatial distribution of residuals. A) AP1 approach, B) AP1L approach, C) AP2 approach and D) AP2L approach. BRT = boosted regression trees, RF = random forest, and SVR = support vector regression.

378 **3.3 Subdividing soil inventories into mineral and organic subsets (AP2 and AP2L)**

379 As outlined in the sections above, the modelling of SOC content when mineral and organic soils were combined
380 led to a systematic underprediction of soils with higher SOC values by all three algorithms, irrespective of the
381 number of training samples. Therefore, by implementing the AP2 approach with two models one for mineral soils
382 and one for organic soils, a noticeable improvement in the performance of all algorithms was observed (Table
383 S3B), with SVR showing the best error metrics (Fig. 2A6, Fig. 2B6, Fig. 2C6). This meant 34% lower RMSE,
384 30% lower MAE, and 32% lower MAPE than when this algorithm was trained under the AP1 approach with one
385 model for all soils. As the high variability of SOC was initially hard to capture, the subdivision of the dataset
386 provided a range that better represented each soil class. This was particularly beneficial for mineral soils (ranging
387 from 4 g kg⁻¹ to 85 g kg⁻¹) since the number of samples did not reduce drastically (only by 99 samples). Thus, the
388 algorithms could better capture the relationship between SOC and covariates. Consequently, the overall
389 performance improved when the underrepresented soil class was modelled separately. This is in line with the study
390 of Rawlins et al. (2009) that recommends separate modelling of mineral and organic soils.

391 Nonetheless, following the AP2L approach with additional data, the RMSE and MAPE of the algorithms improved
392 by less than 2% compared with AP2 (Table S3E). However, the greatest change was observed in the MAE of SVR
393 with a 2% improvement. Therefore, additional training samples did not greatly influence the performance since
394 the majority of these samples were in mineral soils, while the limiting factor was the high variability of organic
395 soils combined with its low number of samples. However, an improvement was noted in relation to all error metrics
396 of SVR in the AP2L approach. This contrasted with when the training set was enlarged without subdividing the
397 data, i.e. AP1L. Therefore, it further confirmed that it is more important for SVR than for BRT and RF to model
398 the soil classes separately when the training set is enlarged by datasets with similar characteristics.

399 Furthermore, the improvement of the algorithms in AP2 and AP2L was particularly noticeable in their relative
400 residuals. By comparing these results with those from AP1 and AP1L, it was evident that the greatest improvement
401 was observed in the northern region and the spatial distribution of relative residuals was more homogenous
402 throughout the country for all algorithms, but particularly for RF and SVR (Fig. 3 C and D). This is understandable
403 since by subdividing the data, the algorithms can no longer exploit any information from the map of organic soil
404 for spatial variability of SOC in mineral soils. Thus, they obtain information from other covariates for this soil
405 class (Fig. 4 B). Although land use and total nitrogen were still among the most important variables for the
406 algorithms in mineral soils, the importance of the predictors representing the SCORPAN C and P factors increased
407 in the absence of a soil organic map. This was to be expected because north-east Germany, for example, has a
408 continental climate (Roßkopf et al., 2015) and young moraine landscapes, while the north-west has a more oceanic
409 climate (Roßkopf et al., 2015) with old moraine landscapes.

410 It is unsurprising that all the algorithms still relied on the map of organic soil to explain SOC in organic soil class.
411 However, while SVR and RF obtained information from other covariates, the value for variable importance of this
412 map alone was 93% in BRT (Fig. 4 C), which makes this algorithm prone to greater errors, as can be seen in its
413 error metrics (Table S2). Similar to mineral soils, the order of covariates was different between the algorithms in
414 organic soils. In other words, in AP1 the three algorithms obtained almost all the information from the map of
415 organic soil, land use and total nitrogen in that order of importance. In contrast, after subdividing the data, the
416 algorithms differed from each other by the order of covariates in their variable importance (Fig. 4).

417 A comparison of the error metrics of each soil class in AP2 with its counterpart in AP2L revealed that the additional
 418 1177 samples had a minor influence on the performance (from zero to a maximum of 2%) of the algorithms in
 419 mineral soils (Table S2). These results indicated that the German Agricultural Soil Inventory offers a good
 420 representation of the spatial variability of SOC in mineral soil under agricultural use throughout the country and
 421 that the inclusion of more sample points did not provide additional information about SOC variability in this soil
 422 class.

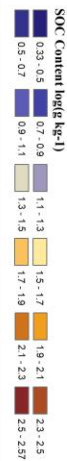
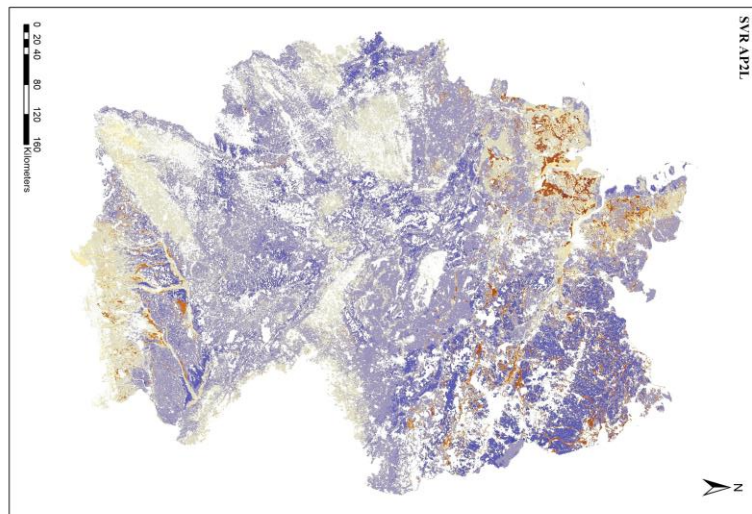
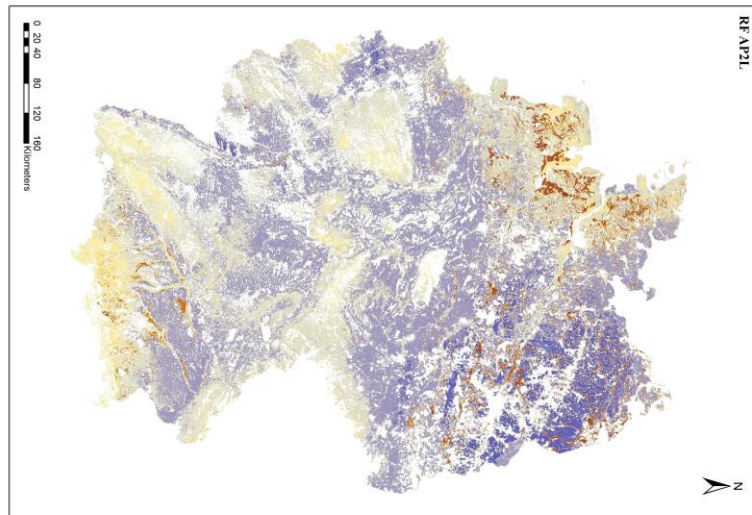
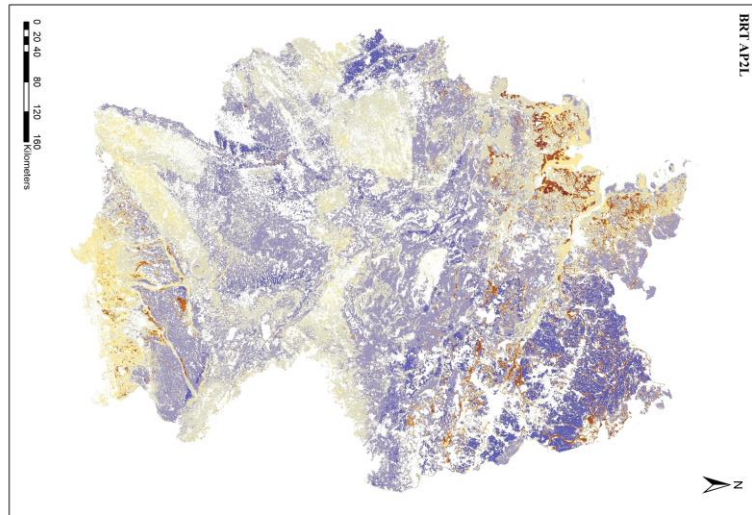
423 However, 46 additional organic soil samples from the LUCAS dataset improved the MAPE and MAE by 12% and
 424 6% for SVR, by 10%, and 4% for RF, and by 7% and 2% for BRT, respectively, but the RMSE of the three
 425 algorithms was improved by less than 2%. Thus, additional organic samples mainly influenced the average
 426 magnitude of the error. This could be explained by organic soils having a wide range of SOC and the number of
 427 samples being limited. Thus, the addition of LUCAS data to the training set gave the algorithms more information
 428 about spatial variability of SOC in this soil class. Despite this limitation, SVR had the best overall performance
 429 among the algorithms in AP2 and AP2L. It should be noted that training samples must span the complexity of the
 430 parameter space in order for the model to be able to match the training data effectively and generalise unseen data.
 431 A small sample size can therefore negatively influence the predictive power of the algorithms. This complexity
 432 can be addressed by structural risk minimisation (SRM) (Al-Anazi and Gates, 2012). Implementation of SRM
 433 makes SVR capable of performing well in such datasets. Other studies have compared the performance of
 434 algorithms on different sample sizes in predicting soil properties and shown that SVR is one of the best choices, if
 435 not the best, when the number of samples is a limiting factor (Al-Anazi and Gates, 2012; Khaledian and Miller,
 436 2020). In contrast, in a study by Zhou et al. (2021), 150 samples with different sets of covariates at different
 437 resolutions were used to compare RF, BRT and SVR to predict SOC content in Switzerland. Their results showed
 438 that the best-performing algorithm varied depending on the resolution and covariates. However, the best
 439 performance throughout all scenarios was obtained by BRT. The discrepancy between their results and the results
 440 of the present study may be due to the parameter-tuning method of the algorithms, as they only used grid search,
 441 or other factors, including the spatial distribution of samples or the chosen set of covariates.

442 **Table 2: Mean of error metrics of the three models for each approach.**

Approach	Mean RMSE (g kg ⁻¹)	Mean MAE (g kg ⁻¹)	Mean MAPE (%)
AP1	32.6	12.3	49.0
AP1L	32.1	12.1	46.9
AP2	21.6	8.8	34.4
AP2L	21.3	8.7	34.3

443 Overall, the change in performance across different sample sizes, different algorithms and different approaches
 444 (Table S3) indicated that the most important aspect of modeling SOC content of German agricultural topsoil is a
 445 two-model approach. Although combining soil inventories for more training samples can possibly improve model
 446 performance, the effect was not noticeable compared to when each soil class was predicted by its dedicated model
 447 (Table S3B and Table S3D). The advantage of two-model approach can also be seen in the average error metrics
 448 of the three models (Table 2). While the average RMSE of the models reduces by less than 1 g kg⁻¹ after enlarging
 449 the training set, the same error metrics reduces by more than 10 g kg⁻¹ in AP2 and AP2L (Table 2). Therefore, it

450 is also recommended to consider the two-model approach in soil-landscape settings similar to Germany or
451 situations where one-model approach cannot have good predictive performance.



452

453 **Figure 7: Spatial prediction of SOC content (g kg⁻¹) of German agricultural soils based on the two-model approach for**
 454 **the three algorithms (BRT AP2L, RF AP2L, SVR AP2L). BRT = boosted regression trees, RF = random forest, and**
 455 **SVR = support vector regression. It is important to note that the provided spatial prediction of SOC content must not**
 456 **be used to identify the organic soils of Germany or to determine their spatial distribution.**

457 The map of organic soil was used to spatially distinguish each soil class to map the SOC content of the class by its
458 corresponding model. Figure 7S5 shows the spatial distribution of SOC content using the AP2L approach for the
459 three algorithms. Although SVR captured a wider range of SOC, 2 g kg⁻¹ to 371.5 g kg⁻¹, than BRT, 8 g kg⁻¹ to
460 341.1 g kg⁻¹, and RF, 7.7 g kg⁻¹ to 354.6 g kg⁻¹, all three algorithms showed a relatively similar distribution of SOC
461 content across the country ~~particularly in mineral soils. In mineral soils, a higher SOC content is mainly found in~~
462 ~~the northwest and the south, particularly for BRT and RF, while the northeast of the country shows a lower SOC~~
463 ~~content. As explained in the previous sections, one of the main reasons for this distribution is land use since high~~
464 ~~SOC content regions are mainly under grassland while low SOC content regions are under use as cropland.~~ As
465 shown in Figure 7S5, organic soils are mainly distributed in the north. ~~Most bog peat soils are located in the~~
466 ~~northwest, while fen peat soils can be found both in the northwest and in the northeast. These soils are mostly bogs~~
467 ~~in the northwest and fens in the northeast (Roßkopf et al., 2015). There is also a small distribution of organic~~
468 ~~soil. Smaller areas of all types of organic soils can be found in the moraine landscapes and the foothills of Alps in~~
469 the south. ~~It is important to note that the provided spatial prediction of SOC content must not be used to identify~~
470 ~~the organic soils of Germany or to determine their spatial distribution. One reason is low sample size of organic~~
471 ~~soils and the systematic underestimation of their SOC content, which leads to an underestimation of their spatial~~
472 ~~extent. Furthermore, the present analysis is limited to the topsoil, but organic soils might have been mixed with~~
473 ~~mineral soil, i.e. due to deep ploughing, or feature a mineral soil cover. Thus, organic soils might be present despite~~
474 ~~having a mineral topsoils. Finally, some of the data used for the derivation of the map of organic soils are subjected~~
475 ~~to improvement and thus modifications in spatial distribution are expected. Therefore, this study cannot nor intend~~
476 ~~to delineate or classify organic soils. In mineral soils, a higher SOC content is mainly found in northwest and south~~
477 ~~of the country. As explained in the previous sections, one of the main reasons for this distribution is land use since~~
478 ~~these regions are mainly under grassland while low SOC content regions are found under cropland.~~

479 **4 Conclusions**

480 The three algorithms most commonly used in DSM were applied to predict the SOC content of German agricultural
481 soils under different approaches. Suitable tuning strategies for each algorithm ensured optimum parameter tuning
482 and made their performance truly comparable. Machine learning was shown to be powerful at modelling SOC on
483 a national scale. However, the study showed that separate modelling of mineral and organic soils was a better
484 approach for modelling SOC compared with just one model. Thus, this approach takes priority over the choice of
485 algorithm and number of training samples. Further testing of this approach is recommended in countries and
486 regions that cover both of these soil classes. Nonetheless, SVR had a better performance than RF and BRT, except
487 when the number of samples in training was increased by additional dataset. This was disadvantageous for SVR
488 and advantageous for BRT unless mineral and organic soils were modelled separately. In general, increasing the
489 number of training samples led to limited improvement of performance. Therefore, this approach should be
490 adopted giving consideration of the algorithm and the characteristics of the data. Furthermore, the better
491 performance of SVR compared with that of RF and BRT was particularly highlighted when predicting SOC in
492 organic soils. The good performance of SVR suggests that this algorithm should therefore be taken into greater
493 account in DSM.

494 **Data availability**

495 The soil data used in this study are publicly available via: <https://doi.org/10.3220/DATA20200203151139> and
496 <https://esdac.jrc.ec.europa.eu/content/lucas-2009-topsoil-data>

497 **Author contribution**

498 AS and AD conceptualised and developed the methodology of the presented work, with input from ML.AS
499 gathered the predictors with contributions from AD. AS executed the programming, testing of existing code
500 components, formal analysis and visualisation. AG contributed to the programming. The preparation of the paper
501 was done by all authors.

502 **Competing interests**

503 The authors declare that they have no conflict of interest except the author AD is a member of the journal's
504 editorial board .

505 **Acknowledgements**

506 This work is part of the SoilSpace3D-DE project. The LUCAS topsoil dataset used in this work was made available
507 by the European Commission through the European Soil Data Centre managed by the Joint Research Centre (JRC);
508 <http://esdac.jrc.ec.europa.eu/>.

509

510

511 **References**

- 512 Al-Anazi, A. F. and Gates, I. D.: Support vector regression to predict porosity and permeability: Effect of sample
513 size, *Comput. Geosci.*, 39, 64–76, <https://doi.org/10.1016/j.cageo.2011.06.011>, 2012.
- 514 Arrouays, D., Jolivet, C., Boulonne, L., Bodineau, G., Saby, N., & Grolleau, E.: A new projection in France: a
515 multi-institutional soil quality monitoring network, *Comptes Rendus l'Académie d'Agriculture Fr.*, 88, 93–103,
516 2002.
- 517 Awad, M. and Khanna, R.: Support Vector Regression, in: *Efficient Learning Machines*, Apress, Berkeley, CA,
518 67–80, https://doi.org/10.1007/978-1-4302-5990-9_4, 2015.
- 519 Ballabio, C., Panagos, P., and Monatanarella, L.: Mapping topsoil physical properties at European scale using the
520 LUCAS database, *Geoderma*, 261, 110–123, <https://doi.org/10.1016/j.geoderma.2015.07.006>, 2016.
- 521 Ballabio, C., Lugato, E., Fernández-Ugalde, O., Orgiazzi, A., Jones, A., Borrelli, P., Montanarella, L., and
522 Panagos, P.: Mapping LUCAS topsoil chemical properties at European scale using Gaussian process regression,
523 *Geoderma*, 355, 113912, <https://doi.org/10.1016/j.geoderma.2019.113912>, 2019.
- 524 Battineni, G., Chintalapudi, N., and Amenta, F.: Machine learning in medicine: Performance calculation of
525 dementia prediction by support vector machines (SVM), *Informatics Med. Unlocked*, 16, 100200,
526 <https://doi.org/10.1016/j.imu.2019.100200>, 2019.
- 527 Behrens, T. and Scholten, T.: Digital soil mapping in Germany - A review, *J. Plant Nutr. Soil Sci.*, 169, 434–443,
528 <https://doi.org/10.1002/jpln.200521962>, 2006.
- 529 Behrens, T., Förster, H., Scholten, T., Steinrücken, U., Spies, E. D., and Goldschmitt, M.: Digital soil mapping
530 using artificial neural networks, *J. Plant Nutr. Soil Sci.*, 168, 21–33, <https://doi.org/10.1002/jpln.200421414>, 2005.
- 531 Belon, E., Boisson, M., Deportes, I. Z., Eglin, T. K., Feix, I., Bispo, A. O., Galsomies, L., Leblond, S., and Guellier,
532 C. R.: An inventory of trace elements inputs to French agricultural soils, *Sci. Total Environ.*, 439, 87–95,
533 <https://doi.org/10.1016/j.scitotenv.2012.09.011>, 2012.
- 534 Bhadra, T., Bandyopadhyay, S., and Maulik, U.: Differential Evolution Based Optimization of SVM Parameters
535 for Meta Classifier Design, *Procedia Technol.*, 4, 50–57, <https://doi.org/10.1016/j.protcy.2012.05.006>, 2012.
- 536 Borrelli, P., Van Oost, K., Meusburger, K., Alewell, C., Lugato, E., and Panagos, P.: A step towards a holistic
537 assessment of soil degradation in Europe: Coupling on-site erosion with sediment transfer and carbon fluxes,
538 *Environ. Res.*, 161, 291–298, <https://doi.org/10.1016/j.envres.2017.11.009>, 2018.
- 539 Breiman, L.: *Randon Forests*, 1–35, 1999.
- 540 de Brogniez, D., Ballabio, C., Stevens, A., Jones, R. J. A., Montanarella, L., and van Wesemael, B.: A map of the
541 topsoil organic carbon content of Europe generated by a generalized additive model, *Eur. J. Soil Sci.*, 66, 121–
542 134, <https://doi.org/10.1111/ejss.12193>, 2015.
- 543 Burke, I. C., Yonker, C. M., Parton, W. J., Cole, C. V., Flach, K., and Schimel, D. S.: Texture, Climate, and
544 Cultivation Effects on Soil Organic Matter Content in U.S. Grassland Soils, *Soil Sci. Soc. Am. J.*, 53, 800–805,
545 <https://doi.org/10.2136/sssaj1989.03615995005300030029x>, 1989.
- 546 Camera, C., Zomeni, Z., Noller, J. S., Zissimos, A. M., Christoforou, I. C., and Bruggeman, A.: A high resolution
547 map of soil types and physical properties for Cyprus: A digital soil mapping optimization, *Geoderma*, 285, 35–49,
548 <https://doi.org/10.1016/j.geoderma.2016.09.019>, 2017.
- 549 Carter, B. J. and Ciolkosz, E. J.: Slope gradient and aspect effects on soils developed from sandstone in
550 Pennsylvania, *Geoderma*, 49, 199–213, [https://doi.org/10.1016/0016-7061\(91\)90076-6](https://doi.org/10.1016/0016-7061(91)90076-6), 1991.
- 551 Castaldi, F., Hueni, A., Chabrilat, S., Ward, K., Buttafuoco, G., Bomans, B., Vreys, K., Brell, M., and van
552 Wesemael, B.: Evaluating the capability of the Sentinel 2 data for soil organic carbon prediction in croplands,
553 *ISPRS J. Photogramm. Remote Sens.*, 147, 267–282, <https://doi.org/10.1016/j.isprsjprs.2018.11.026>, 2019.
- 554 Chapman, S. J., Bell, J. S., Campbell, C. D., Hudson, G., Lilly, A., Nolan, A. J., Robertson, A. H. J., Potts, J. M.,
555 and Towers, W.: Comparison of soil carbon stocks in Scottish soils between 1978 and 2009, *Eur. J. Soil Sci.*, 64,
556 455–465, <https://doi.org/10.1111/ejss.12041>, 2013.
- 557 Cherkassky, V. and Ma, Y.: *FL Methods New Genetic Technology.pdf*, 17, 113–126, 2004.
- 558 Conrad, O., Bechtel, B., Bock, M., Dietrich, H., Fischer, E., Gerlitz, L., Wehberg, J., Wichmann, V., and Böhner,

559 J.: System for Automated Geoscientific Analyses (SAGA) v. 2.1.4, *Geosci. Model Dev.*, 8, 1991–2007,
560 <https://doi.org/10.5194/gmd-8-1991-2015>, 2015.

561 Deng, S., Wang, C., Wang, M., and Sun, Z.: A gradient boosting decision tree approach for insider trading
562 identification: An empirical model evaluation of China stock market, *Appl. Soft Comput. J.*, 83, 105652,
563 <https://doi.org/10.1016/j.asoc.2019.105652>, 2019.

564 DWD Climate Data Center (CDC): Multi-annual grids of annual sunshine duration over Germany 1981-
565 2010, version v1.0, 2017.

566 DWD Climate Data Center (CDC): Multi-annual grids of monthly averaged daily minimum air temperature (2m)
567 over Germany, version v1.0, 2018a.

568 DWD Climate Data Center (CDC): Multi-annual grids of number of summer days over Germany, version v1.0,
569 2018b.

570 DWD Climate Data Center (CDC): Multi-annual grids of precipitation height over Germany 1981-2010, version
571 v1.0, 2018c.

572 Environmental Systems Research Institute (ESRI): ArcGIS 10.2 for Desktop, 2013.

573 European Union Copernicus Land Monitoring Service, and E. E. A. (EEA): European Digital Elevation Model
574 (EU-DEM), Version 1.1, 2016.

575 Eurostat grid generation tool for ArcGIS: [https://www.efgs.info/information-base/best-practices/tools/eurostat-
576 grid-generation-tool-arcgis/](https://www.efgs.info/information-base/best-practices/tools/eurostat-grid-generation-tool-arcgis/).

577 Federal Agency for Cartography and Geodesy (BKG): Digitales Basis-Landschaftsmodell (Basis-DLM), Leipzig,
578 2019.

579 Federal Institute for Geosciences and Natural Resources (BGR): Geomorphographic Map of Germany
580 (GMK1000), Hanover, 2007.

581 Federal Institute for Geosciences and Natural Resources (BGR): Soil scapes in Germany 1:5,000,000 (BGL5000),
582 Hanover, 2008.

583 Federal Institute for Geosciences and Natural Resources (BGR) and German State Geological Surveys (SDG):
584 Hydrogeological Map of Germany 1:250,000 (HÜK250), Hanover, 2019.

585 Forkuor, G., Hounkpatin, O. K. L., Welp, G., and Thiel, M.: High resolution mapping of soil properties using
586 Remote Sensing variables in south-western Burkina Faso: A comparison of machine learning and multiple linear
587 regression models, *PLoS One*, 12, 1–21, <https://doi.org/10.1371/journal.pone.0170478>, 2017.

588 Friedman, J., Tibshirani, R., and Hastie, T.: Additive logistic regression: a statistical view of boosting (With
589 discussion and a rejoinder by the authors), *Ann. Stat.*, 28, 337–407, <https://doi.org/10.1214/aos/1016120463>, 2000.

590 Friedman, J., Hastie, T., and Tibshirani, R.: *The Elements of Statistical Learning*, second., Springer New York,
591 New York, NY, 158-61 pp., <https://doi.org/10.1007/b94608>, 2009.

592 Friedman, J. H.: Stochastic gradient boosting, *Comput. Stat. Data Anal.*, 38, 367–378,
593 [https://doi.org/10.1016/S0167-9473\(01\)00065-2](https://doi.org/10.1016/S0167-9473(01)00065-2), 2002.

594 Gebauer, A., Ellinger, M., Brito Gomez, V., and Ließ, M.: Development of pedotransfer functions for water
595 retention in tropical mountain soil landscapes: Spotlight on parameter tuning in machine learning, 6, 215–229,
596 <https://doi.org/10.5194/soil-6-215-2020>, 2020.

597 Greenwell, B., Boehmke, B., and Cunningham, J.: Package “gbm” - Generalized Boosted Regression Models,
598 CRAN Repos., 39, 2019.

599 Guevara, M., Olmedo, G. F., Stell, E., Yigini, Y., Aguilar Duarte, Y., Arellano Hernández, C., Arévalo, G., Arroyo-
600 Cruz, C. E., Bolivar, A., Bunning, S., Bustamante Cañas, N., Cruz-Gaistardo, C. O., Davila, F., Dell Acqua, M.,
601 Encina, A., Figueredo Tacona, H., Fontes, F., Hernández Herrera, J. A., Ibelle Navarro, A. R., Loayza, V.,
602 Manueles, A., Mendoza Jara, F., Olivera, C., Osorio Hermosilla, R., Pereira, G., Prieto, P., Alexis Ramos, I., Rey
603 Brina, J. C., Rivera, R., Rodríguez-Rodríguez, J., Roopnarine, R., Rosales Ibarra, A., Rosales Riveiro, K. A.,
604 Schulz, G. A., Spence, A., Vasques, G., Vargas, R., and Vargas, R.: No Silver Bullet for Digital Soil Mapping:
605 Country-specific Soil Organic Carbon Estimates across Latin America, *SOIL Discuss.*, 1–20,
606 <https://doi.org/10.5194/soil-2017-40>, 2018.

- 607 Guio Blanco, C. M., Brito Gomez, V. M., Crespo, P., and Ließ, M.: Spatial prediction of soil water retention in a
608 Páramo landscape: Methodological insight into machine learning using random forest, *Geoderma*, 316, 100–114,
609 <https://doi.org/10.1016/j.geoderma.2017.12.002>, 2018.
- 610 Hawkins, D. M., Basak, S. C., and Mills, D.: Assessing model fit by cross-validation, *J. Chem. Inf. Comput. Sci.*,
611 43, 579–586, <https://doi.org/10.1021/ci025626i>, 2003.
- 612 Hornik, K., Weingessel, A., Leisch, F., and Davidmeyer-projectorg, M. D. M.: Package ‘e1071,’ 2021.
- 613 Hoyle, F. C., Baldock, J. A., and Murphy, D. V.: Soil Organic Carbon – Role in Rainfed Farming Systems, *Rainfed
614 Farming Syst.*, <https://doi.org/10.1007/978-1-4020-9132-2>, 2011.
- 615 Khaledian, Y. and Miller, B. A.: Selecting appropriate machine learning methods for digital soil mapping, *Appl.
616 Math. Model.*, 81, 401–418, <https://doi.org/10.1016/j.apm.2019.12.016>, 2020.
- 617 Kuhn, M. and Johnson, K.: *Applied predictive modeling*, 1st ed., Springer-Verlag, New York, 1–600 pp.,
618 <https://doi.org/10.1007/978-1-4614-6849-3>, 2013.
- 619 Lal, R.: Soil carbon sequestration impacts on global climate change and food security, *Science (80-.)*, 304, 1623–
620 1627, <https://doi.org/10.1126/science.1097396>, 2004.
- 621 Li, T., Zhang, H., Wang, X., Cheng, S., Fang, H., Liu, G., and Yuan, W.: Soil erosion affects variations of soil
622 organic carbon and soil respiration along a slope in Northeast China, *Ecol. Process.*, 8,
623 <https://doi.org/10.1186/s13717-019-0184-6>, 2019.
- 624 Li, X., Ding, J., Liu, J., Ge, X., and Zhang, J.: Digital mapping of soil organic carbon using sentinel series data: A
625 case study of the ebinur lake watershed in xinjiang, *Remote Sens.*, 13, 1–19, <https://doi.org/10.3390/rs13040769>,
626 2021.
- 627 Liang, W., Zhang, L., and Wang, M.: The chaos differential evolution optimization algorithm and its application
628 to support vector regression machine, *J. Softw.*, 6, 1297–1304, <https://doi.org/10.4304/jsw.6.7.1297-1304>, 2011.
- 629 Ließ, M., Gebauer, A., and Don, A.: Machine Learning With GA Optimization to Model the Agricultural Soil-
630 Landscape of Germany: An Approach Involving Soil Functional Types With Their Multivariate Parameter
631 Distributions Along the Depth Profile, *Front. Environ. Sci.*, 9, 1–24, <https://doi.org/10.3389/fenvs.2021.692959>,
632 2021.
- 633 Malik, A. A., Puissant, J., Buckeridge, K. M., Goodall, T., Jehmlich, N., Chowdhury, S., Gweon, H. S., Peyton, J.
634 M., Mason, K. E., van Agtmaal, M., Bland, A., Clark, I. M., Whitaker, J., Pywell, R. F., Ostle, N., Gleixner, G.,
635 and Griffiths, R. I.: Land use driven change in soil pH affects microbial carbon cycling processes, *Nat. Commun.*,
636 9, 1–10, <https://doi.org/10.1038/s41467-018-05980-1>, 2018.
- 637 Martin, M. P., Orton, T. G., Lacerce, E., Meersmans, J., Saby, N. P. A., Paroissien, J. B., Jolivet, C., Boulonne,
638 L., and Arrouays, D.: Evaluation of modelling approaches for predicting the spatial distribution of soil organic
639 carbon stocks at the national scale, *Geoderma*, 223–225, 97–107, <https://doi.org/10.1016/j.geoderma.2014.01.005>,
640 2014.
- 641 McBratney, A. B., Mendonça Santos, M. L., and Minasny, B.: On digital soil mapping, 3–52 pp.,
642 [https://doi.org/10.1016/S0016-7061\(03\)00223-4](https://doi.org/10.1016/S0016-7061(03)00223-4), 2003.
- 643 Meersmans, J., Martin, M. P., Lacerce, E., De Baets, S., Jolivet, C., Boulonne, L., Lehmann, S., Saby, N. P. A.,
644 Bispo, A., and Arrouays, D.: A high resolution map of French soil organic carbon, *Agron. Sustain. Dev.*, 32, 841–
645 851, <https://doi.org/10.1007/s13593-012-0086-9>, 2012a.
- 646 Meersmans, J., Martin, M. P., De Ridder, F., Lacerce, E., Wetterlind, J., De Baets, S., Bas, C. Le, Louis, B. P.,
647 Orton, T. G., Bispo, A., and Arrouays, D.: A novel soil organic C model using climate, soil type and management
648 data at the national scale in France, *Agron. Sustain. Dev.*, 32, 873–888, [https://doi.org/10.1007/s13593-012-0085-
649 x](https://doi.org/10.1007/s13593-012-0085-x), 2012b.
- 650 Minasny, B., McBratney, A. B., Malone, B. P., and Wheeler, I.: *Digital Mapping of Soil Carbon*, Elsevier, 1–47
651 pp., <https://doi.org/10.1016/B978-0-12-405942-9.00001-3>, 2013.
- 652 Mulder, V. L., Lacoste, M., Richer-de-Forges, A. C., Martin, M. P., and Arrouays, D.: National versus global
653 modelling the 3D distribution of soil organic carbon in mainland France, *Geoderma*, 263, 16–34,
654 <https://doi.org/10.1016/J.GEODERMA.2015.08.035>, 2016.
- 655 Padarian, J., Minasny, B., and McBratney, A. B.: *Machine learning and soil sciences: A review aided by machine*

- 656 learning tools, 6, 35–52, <https://doi.org/10.5194/soil-6-35-2020>, 2020.
- 657 Pei, T., Qin, C. Z., Zhu, A. X., Yang, L., Luo, M., Li, B., and Zhou, C.: Mapping soil organic matter using the
658 topographic wetness index: A comparative study based on different flow-direction algorithms and kriging
659 methods, *Ecol. Indic.*, 10, 610–619, <https://doi.org/10.1016/j.ecolind.2009.10.005>, 2010.
- 660 Peterson, B., Ulrich, J., and Boudt, K.: Package ‘DEoptim’, <https://doi.org/10.18637/jss.v040.i06>, 2021.
- 661 Poeplau, C., Bolinder, M. A., Eriksson, J., Lundblad, M., and Kätterer, T.: Positive trends in organic carbon storage
662 in Swedish agricultural soils due to unexpected socio-economic drivers, 12, 3241–3251,
663 <https://doi.org/10.5194/bg-12-3241-2015>, 2015.
- 664 Poeplau, C., Jacobs, A., Don, A., Vos, C., Schneider, F., Wittnebel, M., Tiemeyer, B., Heidkamp, A., Prietz, R.,
665 and Flessa, H.: Stocks of organic carbon in German agricultural soils—Key results of the first comprehensive
666 inventory, *J. Plant Nutr. Soil Sci.*, 183, 665–681, <https://doi.org/10.1002/jpln.202000113>, 2020.
- 667 Prechtel, A., Von Łtzw, M., Schneider, B. U., Bens, O., Bannick, C. G., Kögel-Knabner, I., and Hüttl, R. F.:
668 Organic Carbon in soils of Germany: Status quo and the need for new data to evaluate potentials and trends of soil
669 carbon sequestration, *J. Plant Nutr. Soil Sci.*, 172, 601–614, <https://doi.org/10.1002/jpln.200900034>, 2009.
- 670 Ramifehiarivo, N., Brossard, M., Grinand, C., Andriamananjara, A., Razafimbelo, T., Rasolohery, A.,
671 Razafimahatratra, H., Seyler, F., Ranavoson, N., Rabenarivo, M., Albrecht, A., Razafindrabe, F., and
672 Razakamanarivo, H.: Mapping soil organic carbon on a national scale: Towards an improved and updated map of
673 Madagascar, *Geoderma Reg.*, 9, 29–38, <https://doi.org/10.1016/j.geodrs.2016.12.002>, 2017.
- 674 Rawlins, B. G., Marchant, B. P., Smyth, D., Scheib, C., Lark, R. M., and Jordan, C.: Airborne radiometric survey
675 data and a DTM as covariates for regional scale mapping of soil organic carbon across Northern Ireland, *Eur. J.*
676 *Soil Sci.*, 60, 44–54, <https://doi.org/10.1111/j.1365-2389.2008.01092.x>, 2009.
- 677 Reeves, D. W.: The role of soil organic matter in maintaining soil quality in continuous cropping systems, *Soil*
678 *Tillage Res.*, 43, 131–167, [https://doi.org/10.1016/S0167-1987\(97\)00038-X](https://doi.org/10.1016/S0167-1987(97)00038-X), 1997.
- 679 Ritchie, J. C., McCarty, G. W., Venteris, E. R., and Kaspar, T. C.: Soil and soil organic carbon redistribution on
680 the landscape, 89, 163–171, <https://doi.org/10.1016/j.geomorph.2006.07.021>, 2007.
- 681 Roßberg, D., Michel, V., Graf, R., Neukampf, R.: Definition von Boden-Klima-Räumen für die Bundesrepublik
682 Deutschland, *Nachrichtenblatt des Dtsch. Pflanzenschutzdienstes*, 59, 155–161, 2007.
- 683 Roßkopf, N., Fell, H., and Zeitz, J.: Organic soils in Germany, their distribution and carbon stocks, 133, 157–170,
684 <https://doi.org/10.1016/j.catena.2015.05.004>, 2015.
- 685 Santos, C. E. da S., Sampaio, R. C., Coelho, L. dos S., Bestarsd, G. A., and Llanos, C. H.: Multi-objective adaptive
686 differential evolution for SVM/SVR hyperparameters selection, *Pattern Recognit.*, 110, 107649,
687 <https://doi.org/10.1016/j.patcog.2020.107649>, 2021.
- 688 Schapire, R. E.: The Boosting Approach to Machine Learning: An Overview, 149–171,
689 https://doi.org/10.1007/978-0-387-21579-2_9, 2003.
- 690 Schneider, F., Amelung, W., and Don, A.: Origin of carbon in agricultural soil profiles deduced from depth
691 gradients of C:N ratios, carbon fractions, $\delta^{13}\text{C}$ and $\delta^{15}\text{N}$ values, *Plant Soil*, 460, 123–148,
692 <https://doi.org/10.1007/s11104-020-04769-w>, 2021.
- 693 Smola, A. J. and Schölkopf, B.: A tutorial on support vector regression, *Stat. Comput.*, 14, 199–222,
694 <https://doi.org/10.1023/B:STCO.0000035301.49549.88>, 2004.
- 695 Storn, R. and Price, K.: Differential Evolution - A Simple and Efficient Heuristic for Global Optimization over
696 Continuous Spaces, *J. Glob. Optim.*, 11, 341–359, <https://doi.org/10.1023/A:1008202821328>, 1997.
- 697 Taghizadeh-Toosi, A., Olesen, J. E., Kristensen, K., Elsgaard, L., Østergaard, H. S., Lægdsmand, M., Greve, M.
698 H., and Christensen, B. T.: Changes in carbon stocks of Danish agricultural mineral soils between 1986 and 2009,
699 *Eur. J. Soil Sci.*, 65, 730–740, <https://doi.org/10.1111/ejss.12169>, 2014.
- 700 Tóth, G., Jones, A., and Montanarella, L.: LUCAS Topsoil Survey: Methodology, Data, and Results,
701 <https://doi.org/10.2788/97922>, 2013.
- 702 Tziachris, P., Aschonitis, V., Chatzistathis, T., Papadopoulou, M., and Doukas, I. J. D.: Comparing machine
703 learning models and hybrid geostatistical methods using environmental and soil covariates for soil pH prediction,

704 ISPRS Int. J. Geo-Information, 9, <https://doi.org/10.3390/ijgi9040276>, 2020.

705 Varma, S. and Simon, R.: Bias in error estimation when using cross-validation for model selection, *BMC*
706 *Bioinformatics*, 7, 1–8, <https://doi.org/10.1186/1471-2105-7-91>, 2006.

707 Wadoux, A. M. J. C., Minasny, B., and McBratney, A. B.: Machine learning for digital soil mapping: Applications,
708 challenges and suggested solutions, *Earth-Science Rev.*, 210, <https://doi.org/10.1016/j.earscirev.2020.103359>,
709 2020.

710 Wang, S., Xu, L., Zhuang, Q., and He, N.: Investigating the spatio-temporal variability of soil organic carbon
711 stocks in different ecosystems of China, *Sci. Total Environ.*, 758, <https://doi.org/10.1016/j.scitotenv.2020.143644>,
712 2021.

713 Wang, X., Zhang, Y., Atkinson, P. M., and Yao, H.: Predicting soil organic carbon content in Spain by combining
714 Landsat TM and ALOS PALSAR images, *Int. J. Appl. Earth Obs. Geoinf.*, 92, 102182,
715 <https://doi.org/10.1016/j.jag.2020.102182>, 2020.

716 Ward, K. J., Chabrilat, S., Neumann, C., and Foerster, S.: A remote sensing adapted approach for soil organic
717 carbon prediction based on the spectrally clustered LUCAS soil database, *Geoderma*, 353, 297–307,
718 <https://doi.org/10.1016/j.geoderma.2019.07.010>, 2019.

719 Were, K., Bui, D. T., Dick, Ø. B., and Singh, B. R.: A comparative assessment of support vector regression,
720 artificial neural networks, and random forests for predicting and mapping soil organic carbon stocks across an
721 Afrotropical landscape, *Ecol. Indic.*, 52, 394–403, <https://doi.org/10.1016/j.ecolind.2014.12.028>, 2015.

722 Wiesmeier, M., Spörlein, P., Geuß, U., Hangen, E., Haug, S., Reischl, A., Schilling, B., von Lütow, M., and
723 Kögel-Knabner, I.: Soil organic carbon stocks in southeast Germany (Bavaria) as affected by land use, soil type
724 and sampling depth, *Glob. Chang. Biol.*, 18, 2233–2245, <https://doi.org/10.1111/j.1365-2486.2012.02699.x>, 2012.

725 Wright, M. N. and Ziegler, A.: Ranger: A fast implementation of random forests for high dimensional data in C++
726 and R, *J. Stat. Softw.*, 77, 1–17, <https://doi.org/10.18637/jss.v077.i01>, 2017.

727 Yu, D., Hu, F., Zhang, K., Liu, L., and Li, D.: Available water capacity and organic carbon storage profiles in soils
728 developed from dark brown soil to boggy soil in Changbai Mountains, China, *Soil Water Res.*, 16, 11–21,
729 <https://doi.org/10.17221/150/2019-SWR>, 2021.

730 Zhang, J., Niu, Q., Li, K., and Irwin, G. W.: Model selection in SVMs using Differential Evolution, *IFAC*, 14717–
731 14722 pp., <https://doi.org/10.3182/20110828-6-IT-1002.00584>, 2011.

732 Zhong, Z., Chen, Z., Xu, Y., Ren, C., Yang, G., Han, X., Ren, G., and Feng, Y.: Relationship between soil organic
733 carbon stocks and clay content under different climatic conditions in Central China, 9, 1–14,
734 <https://doi.org/10.3390/f9100598>, 2018.

735 Zhou, T., Geng, Y., Ji, C., Xu, X., Wang, H., Pan, J., Bumberger, J., Haase, D., and Lausch, A.: Prediction of soil
736 organic carbon and the C:N ratio on a national scale using machine learning and satellite data: A comparison
737 between Sentinel-2, Sentinel-3 and Landsat-8 images, *Sci. Total Environ.*, 755,
738 <https://doi.org/10.1016/j.scitotenv.2020.142661>, 2021.

739